
Simulation and Experiment of Electromagnet for High-Speed On-off Valve for Vehicle Shifting System*

Qingjun Yang^{1,*}, Yudong Liu¹, Rui Zhu¹, Qi Mao¹,
Rizhi Dong¹ and Hongxuan Jiang²

¹*Dept. Fluid Control and Automation, Harbin Institute of Technology, Harbin, China*

²*National Key Lab of Vehicular Transmission, China North Vehicle Study Institute, Beijing, China*

E-mail: yqj@hit.edu.cn; yudon_liu@163.com; 354732175@qq.com; 1354463139@qq.com; 940762474@qq.com; hxjiang201@163.com

**Corresponding Author*

Received 09 June 2022; Accepted 21 July 2022;
Publication 17 January 2023

Abstract

The high-speed on-off valve is the core component for adjusting the oil pressure of the pressure reducing valve in the clutch shifting system of engineering vehicles, and its response speed is one of the important indicators to measure its performance. In order to improve the dynamic performance of high-speed on-off valve, the electromagnet with solid magnetic isolation structure was designed and simulated by considering the eddy current loss factor. A high-speed on-off valve electromagnetic actuator with high response speed was obtained. Firstly, the theoretical calculation and verification of the theory were carried out by using the electromagnet design theory, and

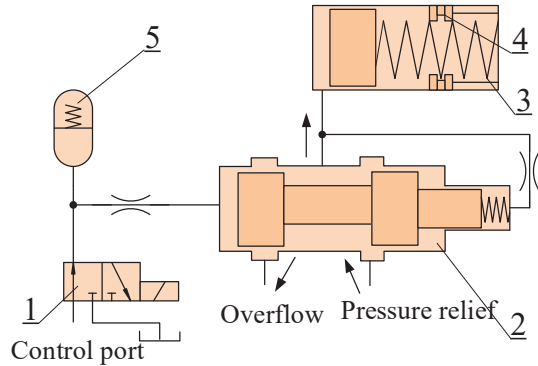
*Basic Product Innovation Plan for Vehicle Power Scientific Research Project (JCCPCX201704).

the theoretical model of the electromagnet was built. Secondly, the electromagnet parameter model was brought into the finite element simulation software ANSYS Electronics to simulate and optimize the static magnetic field and the transient magnetic field respectively. The different structural parameters (guide bush thickness, outer magnetic pole thickness, magnetic isolation structure, armature length) were analyzed. And the effect of the coil parameters (number of strands) on the steady-state electromagnetic force and the dynamic displacement of the armature was analyzed. The values of the structural parameters of the electromagnet were subsequently determined. Finally, the static and dynamic characteristics experiment of the magnetically separated solid electromagnet is designed and processed. The experiment and simulation results are in good agreement. The feasibility of the high-resistance electromagnet structure design and the correctness of the simulation are verified. Reasonable optimization of structural parameters and coil parameters has obvious significance for improving the dynamic characteristics of high-speed on-off valve electromagnets.

Keywords: Clutch shifting system, high-speed on-off valve, electromagnet, responding speed, eddy current loss.

1 Introduction

The electro-hydraulic shifting system of the clutch is an important part of the engineering vehicle transmission system. As shown in Figure 1, the circuit mainly includes high-speed on-off valve, clutch pressure reducing valve, clutch hydraulic cylinder, friction plates and voltage accumulator [1]. As a core component in the shifting circuit, the high-speed on-off valve is used to adjust the opening degree of the clutch pressure reducing valve to realize the combination and separation control of the friction plates in the clutch cylinder [2]. At the same time, high-speed on-off valves are widely used in many fields such as vehicle engines, body suspension control, electronically controlled fuel injection, and anti-lock braking systems. It can directly output digital signals, and has good environmental adaptability. The cost is only about 1/10 of that of servo valves and proportional valves, and the development prospect is very broad [3]. Along with the “Industry 4.0” and “Made in China 2025 Plan”, the new generation of engineering vehicle shifting system puts forward higher requirements on the dynamic performance of high-speed on-off valves: In order to solve the problem of ripple effect in high carrier driving, its response speed needs to be greatly improved [4, 5]. The



1-high speed on-off valve; 2-clutch pressure reducing valve;
3-clutch hydraulic cylinder; 4-clutch friction plates; 5-regulated accumulator

Figure 1 Diagram of clutch electro-hydraulic shift circuit.

electromagnet is used as the internal electro-mechanical drive of the high-speed on-off valve. However, due to the time-consuming and eddy current loss of the flux linkage, the valve opening and closing response speed is limited. The dynamic performance of the electromagnet directly determines the response performance of the high-speed on-off valve. Therefore, designing a high-response electromagnet has become an extremely important part in the development of high-speed on-off valves.

At present, foreign countries have improved the structure of high-speed on-off valve electromagnets, including the Helenoid and Colenoid electromagnets of Britain [6, 7], the US Ford ring multi-stage E-type electromagnets [8, 9], the E-type laminated electromagnets of Japan [10], the Disole electro-magnets of Japan [11], etc. From the perspectives of increasing the magnetized area of moving parts, reducing the weight of the armature, selecting high-saturation magnetic induction materials, and designing the structure of “easy magnetic”, the scholars have improved the response speed of the electromagnetic force and the armature, and the response time can be shortened to about 1ms. Compared with foreign countries, the dynamic response time of most domestic engineering vehicles with high-speed on-off valves can be 5~10 ms, and the type is poor [12–14]. After consulting the literature, the existing research on the optimization design of high-speed on-off valve electromagnets is mostly based on the theoretical formula of common electromagnet design, magnetic circuit segmentation method, etc. [15, 16]. It should be emphasized that the high-speed on-off valve electromagnet and the valve body have strong nonlinearity, so that the dynamic

characteristics of the valve strongly depend on the structural parameters of the electromagnet (guide sleeve thickness, yoke thickness, outer casing thickness, magnetic separation angle, magnetic separation position, armature diameter, etc.) and coil parameters (number of strands). However, some of the structural parameters are not necessarily the optimal values in the empirical formula. It is also necessary to use the finite element method to perform secondary analysis and optimization based on different indicators.

In this paper, the initial calculation and verification of the electromagnet theory were carried out using the electromagnet design theory, and the initial electromagnet theoretical model is built. Then the electromagnet parameter model was established in the finite element software ANSYS Electronics, and the static magnetic field and transient magnetic field were simulated and optimized. By analyzing different structural parameters (guide sleeve thickness, yoke thickness, magnetic separation angle, magnetic separation length, armature length) and coil parameters (number of branches and turns), the optimal structural parameter values based on the shortest response time are obtained. A high-speed electromagnet with magnetic isolation is designed. The magnetically separated solid electromagnet sample was designed and processed, and static and dynamic characteristics experiments were carried out to verify the feasibility of the design of the high-resistance electromagnet and the rationality of the simulation.

2 Structural Design of Electromagnet for High Speed On-off Valve

2.1 Structural Design and Material Selection of Electromagnet for High-speed On-off Valve

In the clutch electro-hydraulic shifting system of the construction vehicle, the high-speed on-off valves output pressure oil to control clutch valve opening degree, and its dynamic characteristics greatly affect the quality of the shift process. The response time requirement of designed high-speed on-off valve is less than 5 ms, driven by a solenoid-type electromagnet, and the recovery method relies on oil hydraulic pressure to recover.

The design specifications for high-speed switching valve electromagnets are as follows:

1. Using conventional PWM control, the voltage value is 24 V;
2. According to the control port flow and pressure demand, determine the working air gap of the armature is 0.3 mm, and the air travel is 1 mm;

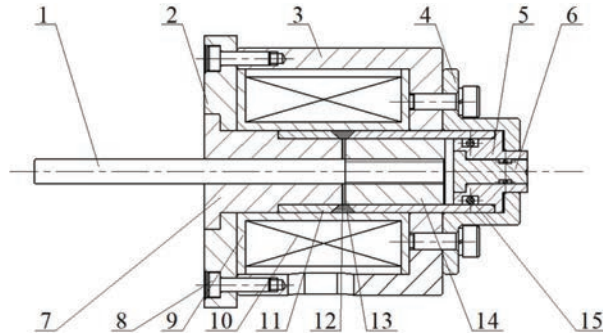


Figure 2 Schematic diagram of high speed switch valve electromagnet.

3. The designed high-speed on-off valve is a normally open ball valve. When the electromagnet is de-energized, the ball valve core is driven by the oil supply pressure. After preliminary calculation, the electromagnetic attraction of the armature under the initial air gap should be greater than 15N;
4. The ambient temperature of the designed valve is about 40°C, and the coil is allowed to rise to 120°C.

The schematic diagram of the high-speed switching valve electromagnet is shown in Figure 2. It is mainly composed of armature push rod 1, upper magnetic yoke 2, shell and lower magnetic yoke 3, fixed end cover 4, rear plug sleeve 5, rear plug core 6, pole shoe 7, bolt 8, coil skeleton 9, double coil 10, guide sleeve 11, limit plate 12, magnetic isolation ring 13, armature 14 and sealing ring 15. One end of the armature putter 1 is threaded with the armature, and the other end acts on the ball valve core.

According to the existing soft magnetic materials in China and abroad, the internal magnetic conductive material of the electromagnet is determined to be industrial pure iron DT4 with high saturation magnetic induction strength. The magnetic isolation ring, the rear blocking core, the rear blocking sleeve and the fixed end cover are austenitic stainless steel 316. The coil frame material is epoxy phenolic glass cloth, and the limit piece is made of copper H62.

2.2 Parameter Design of the Initial Structure of the Electromagnet

American scholar Roters proposed the “structural factor” method for the optimal design of electromagnets: when the electromagnet is in the initial

working air gap, the steady-state electromagnetic attraction and the air gap magnetic induction meet the following formula [15]:

$$K_{\Phi} = \frac{\sqrt{F_{\delta}/10}}{\delta_c} \quad (1)$$

where F_{δ} is the initial working air gap position electromagnetic force, N; δ_c is the working air gap length, mm.

By substituting the above conditions, $K_{\Phi} = 46.5$ can be obtained, and the air gap magnetic induction intensity can be estimated $B_{\delta} = 105000Gs = 1.05T$ from the $B_{\delta} = f(K_{\Phi})$ curve in the electromagnetic design theory.

The steady-state electromagnetic suction can be expressed as [15]:

$$F_{\delta} = 0.31B_{\delta}^2d_{a1}^2 \frac{d_{a1}^2 + 2.5\delta_1^2}{(d_{a1} + 0.74\delta_1)^2} \times 10^6 \quad (2)$$

where δ_1 is the sum of the length of the working air gap and the limiting piece, mm; d_{a1} is the effective diameter of the armature, mm. Under the above conditions, the d_{a1} value is 7.4 mm.

Considering the magnetic pressure drop outside the non-operating air gap, the magnetic potential can be expressed as:

$$IN = 1.25\Phi_{\delta}R_{\delta} \quad (3)$$

where $\Phi_{\delta}R_{\delta}$ represents the magnetic pressure drop at the working air gap, A.

The magnetic resistance, armature diameter and working air gap meet the following formula:

$$\frac{1}{R_{\delta}} = \mu_0 \left(\frac{\pi d_{a1}^2}{4\delta_1} + 0.5d_{a1} \right) \quad (4)$$

By combining Equations (3) and (4), the total magnetic potential of the magnetic circuit can be obtained as 441A.

The length of the coil is determined by the heating equation of the coil:

$$\theta = \frac{\rho_x p}{2\mu_m f_k b_{xq}} \left(\frac{IN}{l_{xq}} \right)^2 \quad (5)$$

where μ_m represents the heat dissipation coefficient of the coil, $W/cm^2 \times ^\circ C$; p represents the duty cycle; b_{xq} represents the coil width, mm; l_{xq} represents the coil length, mm; and f_k represents the filling factor, and it can be obtained as 19 mm.

The cross-sectional area of a single copper wire is obtained from the voltage equation:

$$U = IR_x = IN\rho_x \frac{\pi D_x}{q_x} \quad (6)$$

where D_x is the average coil diameter, mm; U is the coil voltage, V; R_x is the coil resistance, Ω ; ρ_x is the resistivity, $\Omega \times \text{mm}^2/\text{m}$.

The cross-sectional diameter of the wire can be determined based on the cross-sectional area of the wire:

$$q_x = \frac{\pi d_x^2}{4} \quad (7)$$

By combining (5) and (6), the diameter of the copper cross section of a single wire is 0.19 mm. With reference to the enameled wire standard, the diameter of the enameled wire is $d = 0.22$ mm. The coil turns can be estimated from the coil length, width and enameled wire diameter:

$$N = mn = \frac{l_{xq}b_{xq}}{d^2} \quad (8)$$

From the above conditions, the initial number of turns is 2080 turns. The coil resistance is obtained from:

$$R = \rho \times \frac{4D_x}{d_x^2} N \quad (9)$$

The calculated resistance is 110 Ω .

From the above conditions, the initial number of turns is 2080 turns.

Then check the temperature rise of the solenoid coil:

$$\theta = \frac{U^2}{R\mu_m S} \leq \theta_0 \quad (10)$$

In the formula, S represents the heat dissipation area of the coil, mm^2 ; θ_0 represents the allowable temperature rise, $^{\circ}\text{C}$. The verified temperature rise is 111.4°C , which is within the allowable temperature rise range. The initial structural parameters of the high-speed on-off valve electromagnet can be obtained from the design of the electromagnet theory as shown in Table 1.

The above calculation results preliminarily determined the structural parameters and coil parameters of the high-speed on-off valve electromagnet, and checked the coil temperature rise. However, the guide sleeve thickness, armature length, magnetic isolation structure, and the number of coils are

Table 1 Table of structural parameters of electromagnet

Parameters	Values	Unit
Armature diameter d_a	8	mm
Coil outer diameter D_c	23	mm
Coil inner diameter d_c	12.4	mm
Wire section diameter d_x	0.19	mm
Enameled wire diameter d	0.22	mm
Coil length l_{xq}	19.0	mm
Coil width b_{xq}	5.3	mm
Number of coil turns N	2080	tr

just empirical ranges, and their effects on the static electromagnetic force and the armature transient displacement characteristics cannot be accurately reflected. Therefore, finite element software is needed to analyze the static and dynamic magnetic fields of electromagnets. Find the optimal structural and working parameter values based on the shortest response time.

3 Electromagnetic Simulation and Optimization of Electromagnets

In order to obtain greater armature motion acceleration and shorten the response time of the electromagnet, on the one hand, it is necessary to obtain an increase in electromagnetic force under the same volume conditions to ensure a large moving speed; on the other hand, it is necessary to analyze the transient excitation process of the armature. Therefore, based on the finite element software ANSYS Electronics, a simulation model of the static magnetic field and the transient magnetic field of the electromagnet is established. The analysis and optimization of the structural parameters and working parameters are based on the improvement of the static electromagnetic force and the reduction of the armature dynamic response time, and the final structural parameters of the electromagnet are determined.

3.1 Simulation and Analysis of Static Magnetic Field of Electromagnet

When modeling a static electromagnet, the vector magnetic potential A is defined to satisfy the following formula:

$$J_z(x, y) = \nabla \times \left(\frac{1}{\mu_0 \mu_r} (\nabla \times A_z(x, y)) \right) \quad (11)$$

In the formula, $A_z(x, y)$ represents the Z-axis component of the vector magnetic potential, T · m; $J_z(x, y)$ represents the current density of the current flowing section, A/m²; μ_r represents relative permeability, H/m; μ_0 represents vacuum permeability, H/m.

To get the coil inductance matrix, the magnetic field energy needs to be analyzed:

$$U_{ij} = \frac{1}{2}LI^2 = \frac{1}{2} \int_{\Omega} B_i \cdot H_i d\Omega \quad (12)$$

In the formula, U_{ij} represents the magnetic field energy, J; I represents the current, A; B_i represents the magnetic induction intensity at that moment, T; H_i represents the magnetic field intensity at the moment, A/m.

The static electromagnetic force is expressed by the principle of virtual work:

$$F = \left. \frac{dW}{ds} \right|_{i=const} = \frac{\partial}{\partial s} \left[\int_V \left(\int_0^H B \cdot dH \right) dV \right] \quad (13)$$

In the formula, W represents the energy storage of the magnetic field of the system, J; i represents the current establishing the magnetic field, and A; s represents the total displacement in the direction of movement, mm.

Considering that the structure of the electromagnet can be regarded as an axisymmetric model, a two-dimensional simulation module is selected in order to effectively shorten the simulation time without changing the simulation accuracy. The material properties that define each structure are shown in Table 2 and substituted into the magnetization curve of industrial pure iron DT4. Selected current source excitation and balloon boundary conditions, $I_N = 441$ A. Considering the need to continue the transient simulation, combining adaptive meshing and manual meshing, the electromagnet model and meshing are shown in Figure 3. Set the side length of the guide sleeve and the housing unit to 0.3 mm; set the side length of the armature unit to 0.8 mm; set the side length of the coil and yoke unit to 1.5 mm.

3.1.1 Effect of guide bushing thickness on static characteristics

The variation curves of the electromagnetic force of different guide bushing thickness are shown in Figure 4.

It can be seen that when the guide bushing thickness increases, the static electromagnetic force of the moving part decreases. When the armature is in the initial working air gap of 0.3 mm and the thickness of the guide sleeve is 3 mm, the initial electromagnetic force is the smallest, which is 9.22N; when the thickness of the guide sleeve is 0.5 mm, the electromagnetic

Table 2 Table of material properties of electromagnet parts

Part Name	Material	
Armature	DT4	
Bushing	Magnetically permeable part	DT4
	Magnetic isolation part	H62
Shell	DT4	
Yoke	DT4	
Coil	Copper	
Coil bobbin	Epoxy phenolic glass cloth	

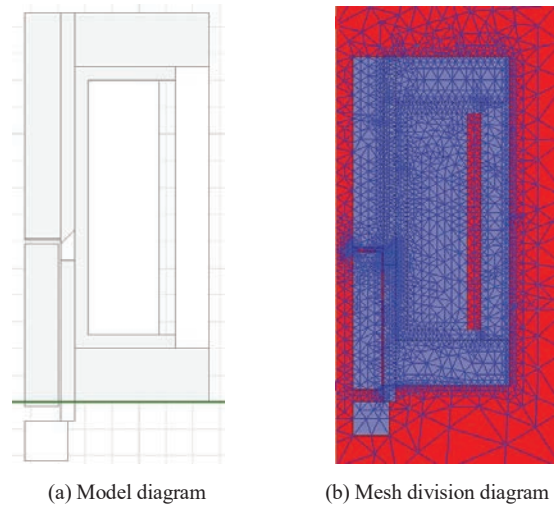


Figure 3 Schematic diagram of high speed switch valve.

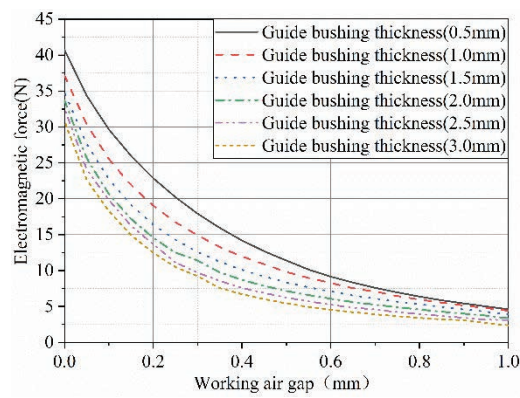


Figure 4 Static electromagnetic force variation of different guide bushing thickness.

force is the largest, which is 17.91N. This phenomenon can be analyzed from the magnetic circuit. When the magnetic field line passes through the internal magnetic circuit of the coil, the magnetic path of the suction place is superimposed by the air gap itself and the guide sleeve at the air gap. An increase in the thickness of the guide sleeve results in a decrease in the magnetic flux passing through the air gap, and an increase in the number of magnetic lines of force passing through the guide sleeve, thereby reducing the steady-state electromagnetic force.

3.1.2 Effects of outer magnetic pole thickness on static characteristics

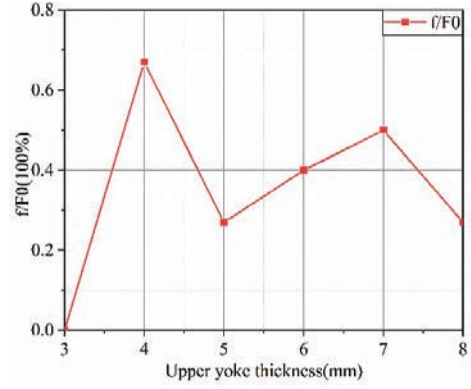
The outer magnetic pole includes an upper magnetic yoke, a lower magnetic yoke and a shell. The effects of different yoke thickness on the electromagnetic force are shown in Figure 5.

It can be seen from the figure that the increase in the thickness of the upper yoke has an effect of increasing the electromagnetic force less than 1%; the increase in the thickness of the lower yoke has a significant effect on the increase of the electromagnetic force, which can increase about 15%. This phenomenon can be analyzed from the perspective of magnetoresistance. When the thickness is 3 mm, the smaller the cross-sectional area there is, the larger the magnetoresistance will be, and the magnetomotive force will be attenuated and the increase of electromagnetic force will be limited. When the thickness is increased to 7 mm, the magnetoresistance decreases, the magnetomotive force attenuates to a decrease, and the armature moving parts gain more magnetomotive force and the electromagnetic force increases. However, the total magnetic potential is constant, so the electromagnetic force does not increase infinitely with the thickness of the yoke. For the same reason, the thickness of the shell has the same result.

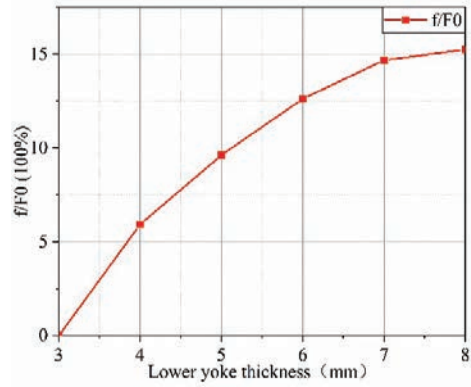
3.1.3 Effects of armature length on static characteristics

The electromagnetic force curve and magnetic flux change of different armature lengths are shown in Figure 6.

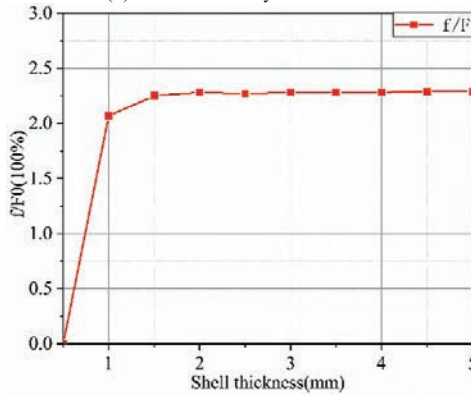
As the armature length increases, the electromagnetic force increases. Due to the change of the armature length, the air gap at the rear end of the armature appears, which reduces the magnetic resistance in the entire magnetic circuit. When the length is increased, the magnetic resistance decreases and the magnetic flux increases. But the magnetic flux cannot increase indefinitely, the armature length reaches a certain value, and the magnetic flux will tend to a fixed value.



(a) Different upper yoke thickness

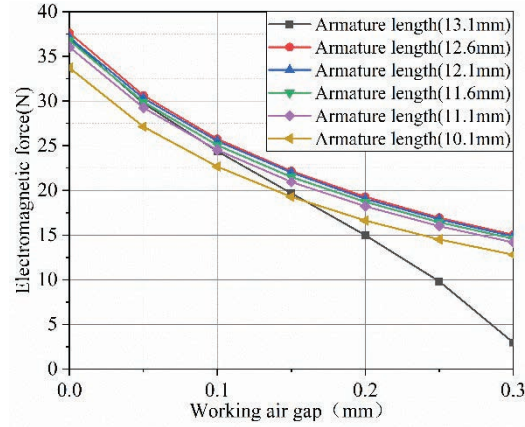


(b) Different lower yoke thickness

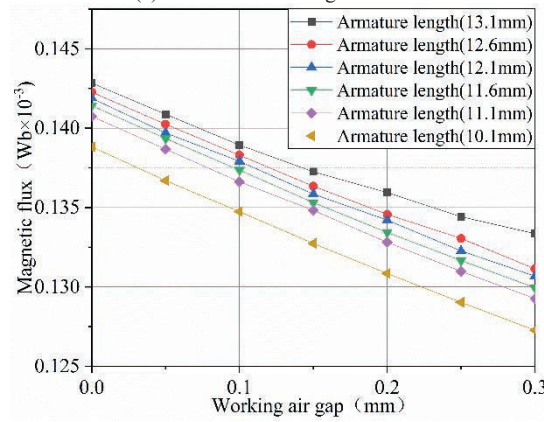


(c) Different shell thickness

Figure 5 Static electromagnetic force variation of different thickness of outer magnetic pole.



(a) Effect of electromagnetic force



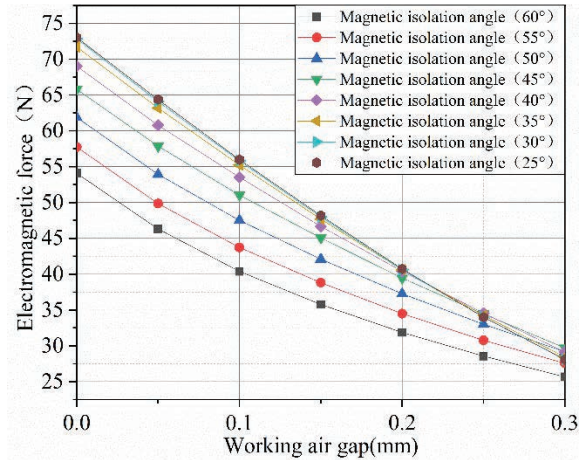
(b) Effect of magnetic flux

Figure 6 Effects of different armature lengths on static properties.

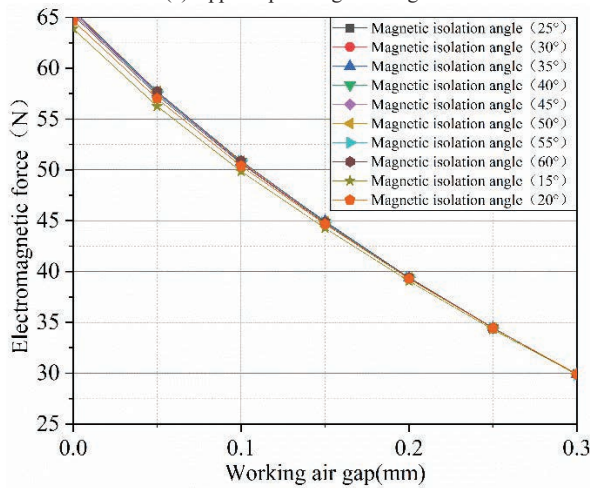
3.1.4 Effects of magnetic isolation structure on static characteristics

The change curves of electromagnetic force at different magnetic isolation angles and magnetic isolation positions are shown in Figures 7 and 8, respectively.

When the upper magnetic separation angle decreases, the electromagnetic force at the initial position increases first and then decreases, and reaches a maximum value at 45°. As the electromagnetic force at the suction point increases, the slope of the electromagnetic force-displacement curve gradually increases. The total electromagnetic force is the vector superposition



(a) Upper septal magnetic angle



(b) Lower magnetic angle

Figure 7 Effects of different magnetic isolation Angle on static characteristics.

of the axial force and the radial force. When the angle is 45° , the initial position of the radial electromagnetic force reaches the maximum value in the axial component. Therefore, an upper magnetic isolation angle of 45° is determined. This magnetic isolation angle obtains the maximum value of the steady-state electromagnetic force at the initial position, which is beneficial to the armature to move with a large acceleration. The effect of the lower

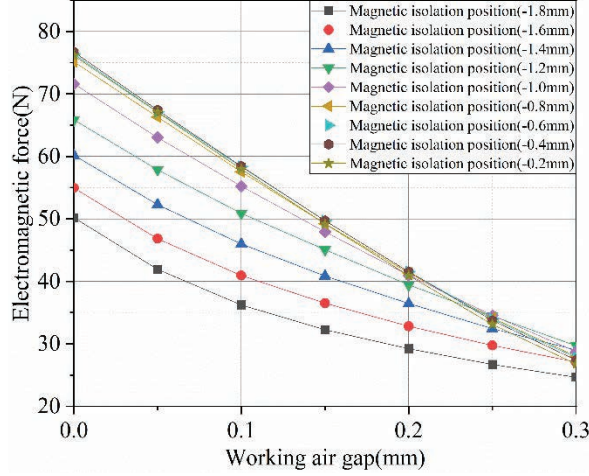


Figure 8 Effects of different magnetic isolation positions on static characteristics.

magnetic isolation angle on the electromagnetic force is not as obvious as the upper magnetic isolation angle.

3.2 Simulation and Analysis of Electromagnetic Transient Magnetic Field

The vector magnetic potential A in the dynamic electromagnetic field satisfies:

$$\nabla \times \frac{1}{\mu} \nabla \times A = J_S - \sigma \frac{\partial A}{\partial t} - \sigma \nabla v - \nabla \times H_c + \sigma v \times \nabla \times A \quad (14)$$

In the formula, H_c represents the coercive force of the permanent magnet, T; v represents the speed of the armature, mm/s; A represents the vector magnetic potential, T·m; J_S represents the true source current density, A/m².

The coil circuit equation of the circuit link:

$$U = i(R + r) + \frac{d\psi}{dt} \quad (15)$$

where U is the voltage across the coil, V; i is the current, A; R is the series resistance of the circuit, Ω ; r is the equivalent resistance of the coil, Ω ; ψ is the flux linkage, Wb.

The static electromagnetic force is expressed by the principle of virtual work:

$$m \frac{d^2x}{dt^2} = F_m - F_p + B \frac{dx}{dt} + kx \quad (16)$$

In the formula, m represents the mass of the moving part, g; x represents the armature displacement, mm; F_p represents the load of the moving part, N; B represents the viscous damping coefficient.

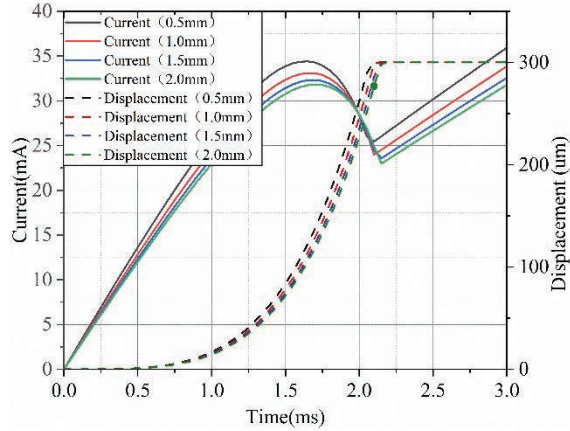
Since the armature is displaced by the electromagnetic force, a band motion domain needs to be added to the model. And the armature is always surrounded by the band motion domain in the whole movement process. The material of the motion domain is set to vacuum. When adding excitation, choose to directly add voltage or current, and external circuit control coils can also be set through the Maxwell Circuit module. When setting in the motion domain, it is necessary to set the movement displacement and mass of the moving body. The armature moves forward along the Z axis, and the maximum displacement is 0.29999 mm.

3.2.1 Effects of guide sleeve thickness on transient characteristics

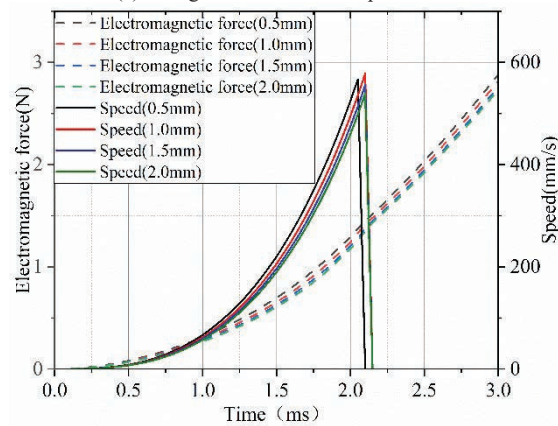
The effects of different guide sleeve thickness on transient characteristics are shown in Figure 9. When the thickness of the guide sleeve is increased from 1 mm to 2 mm, the time consuming increases in the sub-millisecond order. The occurrence of this phenomenon can be analyzed from the perspective of magnetic field lines: the thickness of the guide sleeve does not change much, so the increase in time consumption is relatively small. The number of magnetic lines of force due to magnetic potential is constant, while the guide sleeve and the armature are both magnetically permeable materials and the guide sleeve is located inside the armature. It is closer to the coil so the magnetization effect is higher. As its thickness increases, it means that more magnetic lines of force should have been generated inside the armature. However, as the radial distance increases, it enters the guide sleeve, which makes the degree of magnetization of the guide sleeve higher. The degree of magnetization of the armature is reduced, and it can be seen from the current response and the electromagnetic force response that the growth rate becomes slower, thereby increasing the time consuming.

3.2.2 Effects of armature length on transient characteristics

The effects of different armature lengths on transient characteristics are shown in Figure 10. When the length is 13.1 mm, the armature pull-in



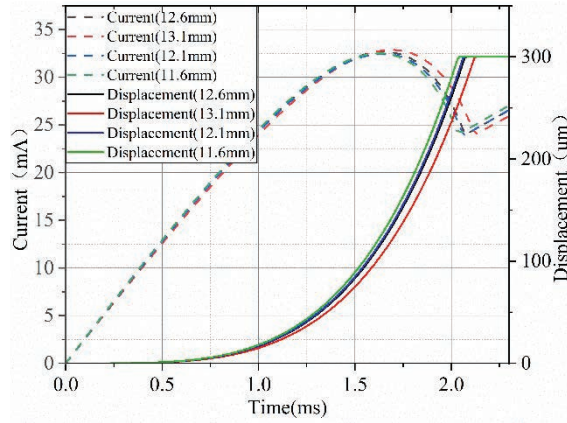
(a) Changes in current and displacement



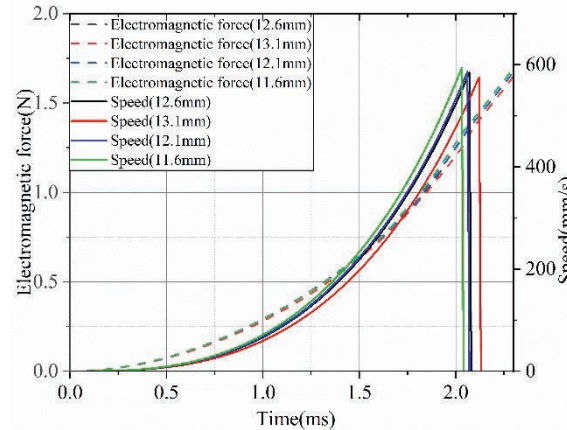
(b) Changes in electromagnetic force and speed

Figure 9 Effects of different guide sleeve thickness on transient characteristics.

takes 2.25 ms; when the length is 11.6 mm, the time is shortened by 8%. From the perspective of magnetization and dynamics of moving parts, an increase in the degree of magnetization is conducive to the increase of the electromagnetic force and the speed of the current increase, and a reduction in the mass is beneficial to the reduction of the inertial force. Therefore, when the length is shortened from 13.1 mm to 11.6 mm, the non-working air gap is increased by 1.5 mm, but the mass is reduced by 0.5 g. After the two effects are superimposed, the mass reduction plays a leading role, so the time consumption is shortened.



(a) Changes in current and displacement

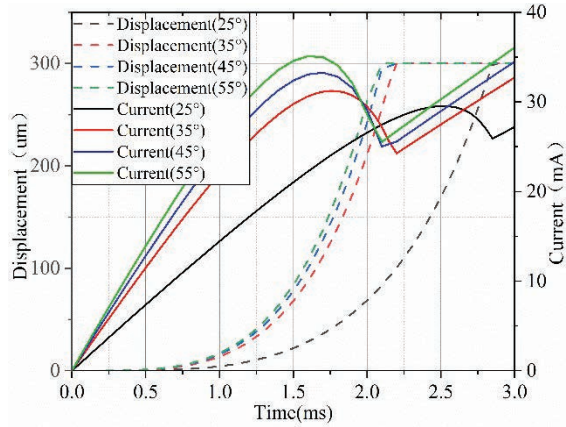


(b) Changes in electromagnetic force and speed

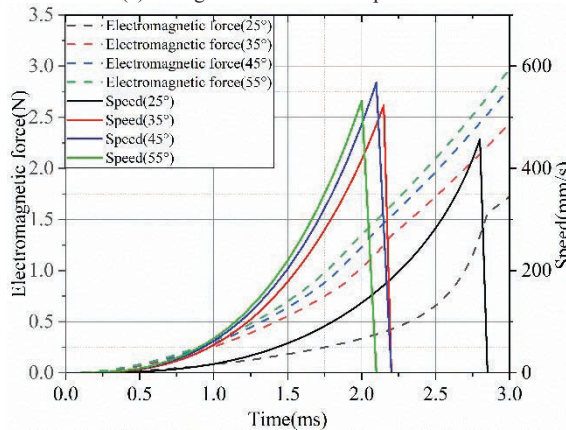
Figure 10 Effects of different armature lengths on transient properties.

3.2.3 Effects of magnetic isolation structure on transient characteristics

Increasing the lower magnetic isolation angle shortens the no-load pull-in time, but the reduction is not consistent. When the angle is increased from 25° to 35° , the response time is shortened from 2.67 ms to 2.35 ms, which is a tenth reduction. When it continues to increase, the time consumption is shortened to the sub-millisecond level, and the effect is reduced. The process can be analyzed from the perspective of magnetic field lines. When the angle is small, no effective magnetic circuit is provided for the magnetic field lines



(a) Changes in current and displacement

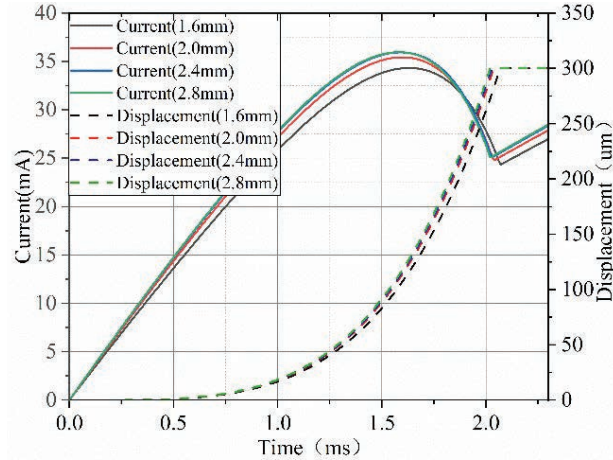


(b) Changes in electromagnetic force and speed

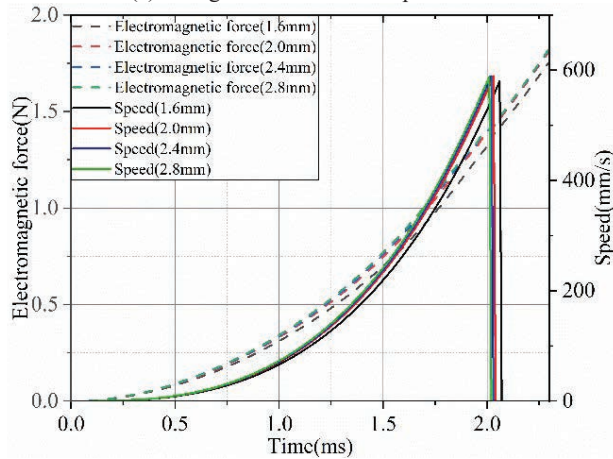
Figure 11 Effects of different magnetic separation angles on transient characteristics.

to pass through the working gap, and the number of magnetic field lines is not large. As the angle increases, the magnetic lines of force of most of the guide sleeves enter the air gap. It can also be seen from the electromagnetic force response curve that the growth rate increases and the time consumption decreases. However, the total number of magnetic lines of force is constant, so the effect of continuing to provide effective magnetic circuit to improve dynamic characteristics will not increase by the same amount.

When the length is 1.6 mm, part of the magnetic field lines directly enter the air gap without passing through the armature, so this part of the magnetic



(a) Changes in current and displacement



(b) Changes in electromagnetic force and speed

Figure 12 Effects of different magnetic isolation lengths on transient characteristics.

field lines does not provide limited magnetic kinetic energy. As the length increases to 2.8 mm, this part of the magnetic field lines are restricted and can only pass through the armature to enter the air gap, which makes the electromagnetic force growth of moving parts increase to a certain extent. However, the number of some magnetic field lines is too small compared with the axial effective magnetic field lines, so the response speed cannot be significantly improved.

3.2.4 Effects of coil strands on transient characteristics

The number of turns is constant, and the effects of different coil strands on transient characteristics are shown in Figure 13. When the number of coils is changed to two, the resistance in the total circuit is reduced to 1/4. It can be seen that the inductance and resistance are also reduced by about 75%. Considering the mutual inductance, the reduction of the inductance is relatively low, and the time constant is basically unchanged. However, since the total resistance is reduced, the stable current is increased. From the response curves of current and electromagnetic force, it can be seen that the growth rate of the two increases significantly. At the time of pull-in, the pull-in current increased from 25 mA to 60 mA. It increased by 1.6 times. And the response time was shortened from 2.01 ms to 1.50 ms, indicating that parallel coils can shorten the response time.

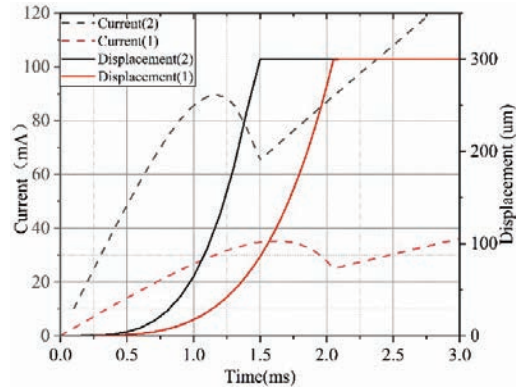
In summary, the structure parameters of electromagnet (thickness of guide sleeve, thickness of outer magnetic pole, length of armature, magnetic isolation structure) and coil parameters (number of strands) are simulated and analyzed. The optimal parameter value based on the shortest response time was determined. As shown in Table 3, a high response magnetically isolated solid electromagnet is obtained.

4 Manufacturing and Testing of Electromagnets

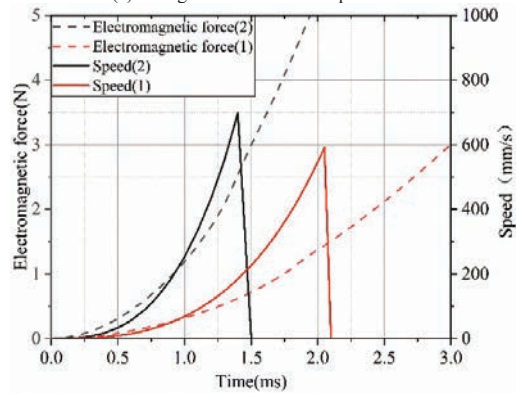
The electromagnet is processed and manufactured, wherein the relevant soft magnetic material is subjected to bright annealing and bluing treatment after the processing is completed to ensure that the internal magnetic characteristics of the soft magnetic material are not affected by the mechanical stress caused by machining. The physical picture of the electromagnet is shown in Figure 14.

The static and dynamic characteristics experiments were performed on the above-mentioned electromagnet test pieces. The dynamic electromagnetic force curves when the force-displacement curve and position are unchanged are shown in Figures 15 and 16.

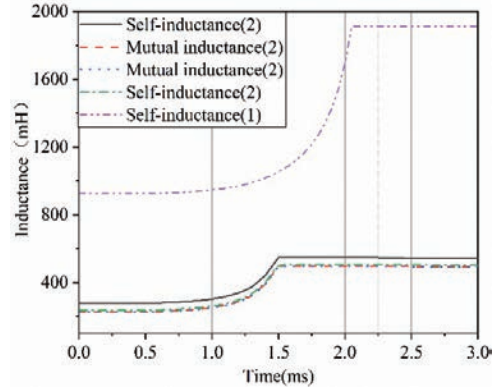
It can be seen from Figure 15 that the steady-state electromagnetic force gradually increases with the decrease of the air gap, and the results obtained from experiments and simulations under the same working air gap conditions are relatively consistent. The electromagnet at the initial air gap position is 60.80N, and the electromagnetic suction at the air gap position of 0.2 mm is 70.20N. The error is within 5%, which verifies the accuracy of the electromagnet simulation model.



(a) Changes in current and displacement



(b) Changes in electromagnetic force and speed



(c) Changes in inductance

Figure 13 Effects of different winding branches on transient characteristics.

Table 3 Table of optimization parameters of electromagnet

Parameters		Values	Unit
Guide bushing thickness		1	mm
Outer magnetic pole thickness	shell	4	mm
	Upper yoke	3	mm
	Lower yoke	6	mm
Armature length		12.1	mm
Magnetic isolation structure	Upper septal magnetic angle	45	°
	Lower magnetic angle	55	°
	Magnetic isolation length	1.8	mm
Coil strands		2	—

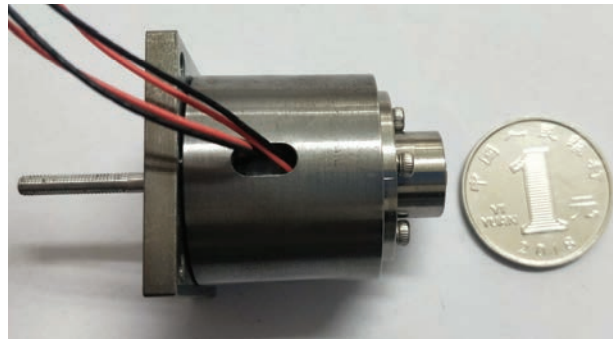


Figure 14 Electromagnet specimen.

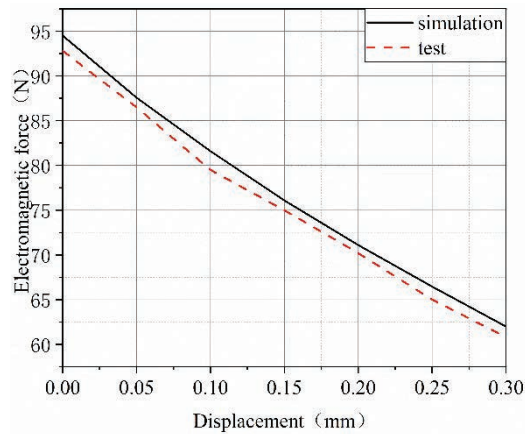
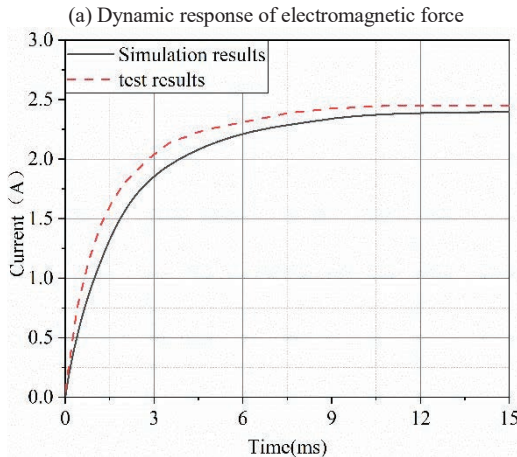
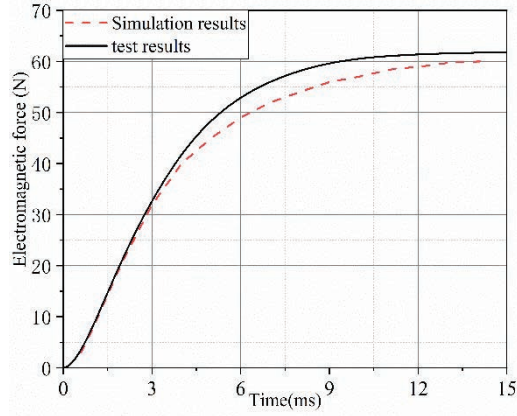


Figure 15 Static electromagnetic force – armature displacement curve of electromagnet.



(b) Dynamic response of current

Figure 16 Dynamic electromagnetic force and current response curve of electromagnet.

5 Conclusion

This paper uses the electromagnet design theory and the finite element software ANSYS Electronics to design the parameter of the high-speed on-off valve electromagnet of the electro-hydraulic gearshift system of the engineering vehicle clutch. It avoids the ambiguity of using only empirical formulas to define parameter range values, which enriches the design method of electromagnets. Aiming at the indicators for improving the static electromagnetic attraction and the dynamic characteristics of the armature, the effects of the structural parameters (the thickness of the guide sleeve, the thickness of the

outer magnetic pole, the length of the armature, and the magnetic isolation structure) and the coil parameters (number of strands) on the electromagnetic force and displacement response were analyzed more comprehensively. It is concluded that reducing the thickness of the guide sleeve, increasing the thickness of the outer magnetic pole and the armature length, and increasing the number of coils can effectively improve the initial electromagnetic suction and response speed. There is an optimal value for the magnetic isolation angle and the magnetic isolation position based on the shortest response time. Test pieces of magnetically isolated solid electromagnets were fabricated and tested. The simulations and the experiment results were relatively consistent. The correctness of the simulation model and the feasibility of the design are verified, which provides ideas for the high-speed on-off valve solenoid of the electro-hydraulic shift system of the engineering vehicle clutch.

References

- [1] Wang Guanhai, Research on Transmission Control System of Automatic Transmission Mechanism Used in High-power vehicles[D]. Harbin Institute of Technology. 2010.
- [2] Sun Chengtong, Ren Haoling. Design and Performance Simulation of Normally Open High Speed Switch Valve Electromagnet[J]. Mechanical Design, 2009, 26(6):10–13.
- [3] Wang Huiyi, GAO Bo. Experimental Study on Action Response of Solenoid Valve in Hydraulic Anti-lock Braking System[J]. Hydraulic & Pneumatics, 2001(9):2–4.
- [4] Zhao Xinxin. Modeling and shift control of automatic transmission for engineering vehicles [D]. University of Science and Technology Beijing, 2015.
- [5] Zhao Keli, Ma Le, Liu Jiyan. Simulation of Intelligent Shift Schedule of Engineering Vehicles[J]. China Journal of Highway and Transport, 2006, 19(5): 123–126.
- [6] Seillyah. Colenoid actuators-further developments in extremely fast acting solenoids[J]. SAE Preprints, 1981 (810462): 1–12.
- [7] Seillyah. Helenoid actuators-a new concept in extremely fast acting solenoids[J]. SAE Preprints, 1979(790119):1–10.
- [8] Schechtermm. Fast response multipole solenoids[J]. SAE, 1983(820203): 846–857.
- [9] Mutaih, Yamasawak. Fundamental operations of a multipolar dis k-solenoid[J]. IEEE T ran sactions on Magnetics, 1995, 31(4):2445–2449.

- [10] Shigeikue, Moriyasug, Kojit. Electromagnetic device with stator displacement regulation: US, 5939811 [P]. 1999-08-17.
- [11] Takeuchik, Shimizum, Okazakik, et al. Fast actuator modeling by finite element method[J]. IEEE Transactions on Magnetics, 1994, 30(6):4284–4286.
- [12] Zhao Jinsong, Zhang Chuanbi, Zhao Zining, Wang Zhipeng, Yao Jing. Static and Dynamic Characteristics of High Speed Switch Digital Valves[J]. China Mechanical Engineering, 2018, 29(02): 145–150+157.
- [13] Li Paixia, Zhang Xiaojun, Liu Keming. Research on Characteristics of High Speed On-Off Valve Based on Double Voltage Drive[J]. Hydraulic & Pneumatic, 2018(07):59–64.
- [14] Liu Xiangyang, Nie Songlin, Li Guanghui. Dynamic Characteristics of Hydraulic Direct Drive High Speed Switch Valve[J]. Journal of Beijing Polytechnic University, 2017, 43(07):1051–1059.
- [15] Zhang Guansheng, Lu Yiguo Tong. Electromagnets and Automatic Electromagnetic Elements [M]. Mechanical Industry Press, 1982.
- [16] Huang Weigang, Wang Xuyong, Wang Xianzheng, Zhong Tingxiu. Study on the Mechanism of Switching Characteristics of High Speed Solenoid Switch Valve[J]. Journal of Shanghai Jiaotong University, 1998(12):40–43.

Biographies



Qingjun Yang received his Ph.D., M.S. and B.S. degrees in mechatronics engineering from Harbin Institute of Technology, China, in 1995, 1997 and 2003, respectively. He has been with the mechatronics engineering at Harbin Institute of Technology since 2003 and promoted to the rank of associate professor in 2006. His research interests include fluid control and flow field

analysis, hydraulic and pneumatic components design, nonlinear control and adaptive control.



Yudong Liu received his M.S. degree in mechatronics engineering from Harbin Institute of Technology, China, in 2019, and received his B.S. degrees in mechanical engineering from Yanshan University, China, in 2017. He is currently pursuing a Ph.D. degree in mechatronics engineering from Harbin Institute of Technology. His research interests include hydraulic components and systems and electro-hydraulic control.



Rui Zhu received his B.S. degree in mechanical engineering from Taiyuan University of Technology, China, in 2017. He is currently pursuing a Ph.D. degree in mechatronics engineering from Harbin Institute of Technology, China. His research interests include quadruped robot, electrohydraulic servo control and nonlinear control.



Qi Mao received his B.S. degree in mechanical engineering from Taiyuan University of Technology, China, in 2018. He is currently pursuing a Ph.D. degree in mechatronics engineering from Harbin Institute of Technology, China. His research interests include heat and mass transfer and microfluidic technology.



Rizhi Dong received his M.S. degree in mechatronics engineering from Northeast Petroleum University, China, in 2018. He is currently pursuing a Ph.D. degree in mechatronics engineering from Harbin Institute of Technology. His research interests include artificial photosynthesis and pipeline vibration.



Hongxuan Jiang received his M.S. degree in mechatronics engineering from Harbin Institute of Technology, China, in 2018. He is currently a researcher at the Transmission Technology Department of the North China Vehicle Research Institute. His research interests include hydraulic systems and electro-hydraulic control.

